

Gamma exposure from building materials – A dose model with expanded gamma lines from naturally occurring radionuclides applicable in non-standard rooms

Peer-reviewed author version

CROYMANS-PLAGHKI, Tom; Leonardi, Federica; Trevisi, Rosabianca; Nuccetelli, Cristina; SCHREURS, Sonja & SCHROEYERS, Wouter (2018) Gamma exposure from building materials – A dose model with expanded gamma lines from naturally occurring radionuclides applicable in non-standard rooms. In: CONSTRUCTION AND BUILDING MATERIALS, 159, p. 768-778.

DOI: 10.1016/j.conbuildmat.2017.10.051

Handle: <http://hdl.handle.net/1942/25403>

# Gamma exposure from building materials – a dose model with expanded gamma lines from Naturally Occurring Radionuclides applicable in non-standard rooms.

Tom Croymans<sup>1</sup>, Federica Leonardi<sup>2</sup>, Rosabianca Trevisi<sup>2</sup>, Cristina Nuccetelli<sup>3</sup>, Sonja Schreurs<sup>1</sup>, Wouter Schroeyers<sup>1</sup>

<sup>1</sup> Hasselt University, CMK, NuTeC, Nuclear Technology - Faculty of Engineering Technology, Agoralaan building H, B-3590 Diepenbeek, Belgium

<sup>2</sup> INAIL (National Institute for Insurance against Accidents at Work) - Research Sector, DiMEILA, Via di Fontana Candida 1 00078 Monteporzio Catone (Rome), Italy

<sup>3</sup> ISS (National Institute of Health), Technology and Health Department, Viale Regina Elena, 299, Rome, Italy

\*Corresponding author: wouter.schroeyers@uhasselt.be

Tel: +3211 29 21 57

\* Hasselt University, NuTeC, CMK, Nuclear Technology - Faculty of Engineering Technology, Agoralaan building H, B-3590 Diepenbeek, Belgium

## Keywords

Euratom Basic Safety Standards; Dose Models; Naturally Occurring Radionuclides; Naturally Occurring Radioactive Materials; Radioactivity; Building materials; Concrete; Inorganic polymers; Alkali-activated materials; External gamma exposure

## Abstract

Building materials are a significant source of gamma rays exposure due to the presence of naturally occurring radionuclides. In order to protect the public from harmful radiation, the European Basic Safety Standards (Council directive 2013/59/Euratom) introduced a one-size-fits-all building(s) (materials) Activity Concentration Index (ACI) based on a limited set of gamma lines. The ACI is considered “as a conservative screening tool for identifying materials that may cause the reference level (i.e. 1 mSv/y) laid down in Article 75(1) to be exceeded”. Regarding calculation of dose, many factors such as density and thickness of the building material, as well as factors relating to the type of building, and the gamma emission data need to be taking into account to ensure accurate radiation protection. In this study the implementation of an expanded set of 1845 gamma lines, related to the decay series of <sup>238</sup>U, <sup>235</sup>U and <sup>232</sup>Th as well as to <sup>40</sup>K, into the calculation method of Markkanen [1], is discussed. The expanded calculation method is called the Expanded Gamma Dose Assessment (EGDA) model. The total gamma emission intensity increased from 2.12 to 2.41 and from 2.41 to 3.04 for respectively the <sup>238</sup>U and <sup>232</sup>Th decay series. In case of <sup>40</sup>K a decrease from 0.107 to 0.1055 is observed. The <sup>235</sup>U decay series is added, having a gamma emission intensity of 3.1. In a standard concrete room, the absorbed dose rates in air (D<sub>A</sub>) per unit of activity concentration of 0.849, 0.256, 1.08, 0.0767 nGy/h per Bq/kg are observed. The use of weighted average gamma lines increased the D<sub>A</sub> with 6.5 % and 1 % for respectively the <sup>238</sup>U and <sup>232</sup>Th decay series. A decrease of 4.5 % is observed in the D<sub>A</sub> of <sup>235</sup>U decay series when using the weighted average gamma lines in comparison to its non-averaged variant. The sensitivity of the EGDA model for density, wall thickness, presence of windows and doors and room size is investigated. Finally, a comparison of the index and dose calculations relevant for the dose

47 assessment within the European legislative framework applicable towards building materials  
48 is performed. In cases where the ACI and density and thickness corrected dose calculation of  
49 Nuccetelli et al. [2] cannot provide guidance, the EGDA allows performing more accurate dose  
50 assessment calculations leading to effective doses which can be several 100  $\mu\text{Sv/y}$  lower.

51

## 52 **1. Introduction**

53

54 Building materials are a significant source of indoor gamma dose [3]. The importance to  
55 address the exposure originating from building materials is underlined in article 75 of the  
56 Euratom basic safety standards (EU-BSS) (Council directive 2013/59/Euratom) which comes  
57 into force in February 2018 [4]. This article states that "*The reference level applying to indoor  
58 external exposure to gamma radiation emitted by building materials, in addition to outdoor  
59 external exposure, shall be 1 mSv per year*". This European legislation was developed to  
60 establish basic standards, applicable in EU member states, for the protection against exposure  
61 of ionising radiation for workers and the general public. In a broader context this legislation  
62 supports several launched initiatives of the European commission for turning waste into a  
63 resource and promoting re-use and recycling with focus on the building industry in the  
64 framework of the Europe 2020 strategy [5–7]. In this context the EU-BSS aims towards a safe  
65 use of by-products, originating from NORM (Naturally Occurring Radioactive Material)-  
66 processing industries, like metallurgical slags, fly and bottom ash, phosphogypsum and red  
67 mud. These residues are used or investigated to use in cement-based matrixes as  
68 supplementary cementitious materials (SCM) on a large scale [8–12]. In addition more and  
69 more research is conducted to use these residues in more CO<sub>2</sub>-friendly cement alternatives,  
70 like inorganic polymers (IPs) [8–10]. This fits with the aim to reduce the usage of primary  
71 resources. It is expected that future building materials used for dwellings will shift more and  
72 more towards these secondary raw materials that can potentially be rich in naturally occurring  
73 radionuclides (NORs): therefore the impact on the external gamma exposure of the use of  
74 these secondary raw materials needs to be assessed [10,13,14].

75

76 In order to assess the impact on external gamma exposure of building materials, different  
77 calculation methods, based on Monte Carlo simulations, integration and simple index and  
78 dose formulas, have been developed in the past [1,15–26]. Different dose assessment  
79 calculations have been developed based on gamma ray attenuation and build-up factors  
80 [1,16,17,22,27]. These calculations allow specifying the physical parameters of the room and  
81 the material it is constructed out, in a straightforward way. The density and wall thickness are  
82 identified as the most critical parameters. Modifying these parameters, for the evaluation of  
83 non-standard rooms, can generate dose rate differences up to 40 % compared to a standard  
84 concrete room [27]. Seeking for a standardized approach, the EU-BSS proposes a screening  
85 index, named Activity Concentration Index (ACI) [2]. This index was originally developed by  
86 Markkanen [1] and is described in the technical guide Radiation Protection (RP)-112 [28]. The  
87 ACI is based on a number of assumptions that are not all necessarily valid. The ACI assumes a  
88 concrete room (400 cm x 500 cm x 280 cm) with a density of 2350 kg/m<sup>3</sup> and thickness of 20  
89 cm for all surfaces (walls, floor and ceiling). In the last years, in order to get a reliable screening  
90 tool, that will allow for a realistic discrimination of building materials, a new density and  
91 thickness corrected index I(pd) was developed by Nuccetelli et al. [2]. The available dose  
92 assessment models focus on the standard composition of concrete, however the increased  
93 usage of residues, which have an *a priori* chemical compositions differing from conventional

94 raw materials (like OPC and gravel), can result in structures with very different compositions.  
95 Some models consequently apply a correction factor to compensate for the different  
96 composition [29]. In addition, disequilibrium in the  $^{238}\text{U}$  and  $^{232}\text{Th}$  decay series chain can be  
97 present for residues from NORM-processing industries. Information regarding disequilibrium  
98 can be valuable for gaining insight into environmental or industrial processes. However, when  
99 dealing with the dose assessments of building materials one should assess how meaningful  
100 the consideration of disequilibrium is. Up to now, to the authors' knowledge, in none of the  
101 existing dose calculations, disequilibrium situations are taken into account. In contrast RP-122  
102 [30] suggests using the highest activity concentration of a radionuclide present in a certain  
103 decay series to specify the activity concentration of that whole decay series. In none of the  
104 existing tools the presence of  $^{235}\text{U}$  and its decay products is considered.

105  
106 The above mentioned calculation methods have in common that they only use a fraction of  
107 the gamma emission lines known today. In practice, this means that often dose models use a  
108 specific set of major gamma lines or that the set of several major gamma lines is reduced to  
109 one or several averaged gamma lines with the gamma intensity as weighing factor. Whereas  
110 the gamma emission intensity of this averaged gamma line is the sum of the individual gamma  
111 emission intensities. This technique is performed to provide simplicity. However progress has  
112 been made in the characterization of the gamma emissions of radionuclides. The Laboratoire  
113 National Henri Becquerel has built an online database providing continuously updated  
114 information on the gamma emission lines of a wide range of radionuclides that allows going  
115 beyond this simplified approach [31]. Implementation of this database into a dose calculation  
116 method allows a more accurate safety assessment to evaluate if construction products can be  
117 used from a radiation protection point of view [2]. Both sample parameters, like density and  
118 composition, as well as room parameters like thickness of the walls, ceiling and floor, number  
119 of walls present, the sample composition of each wall etc. impact the final received dose  
120 [15,27]. An adaptable dose assessment calculation allows taking these parameters into  
121 account.

122  
123 Using an flexible dose or index calculation, in contrast to a screening index, for the evaluation  
124 of building materials fits better with the 1 mSv dose requirement of article 75 of the EU-BSS  
125 [2], in particular when dealing with non-standard room and building material parameters. In  
126 addition the implementation of non-standard room and building material parameters deals  
127 with the requirement of annex VII of the EU-BSS, that states "*The calculation of dose needs to  
128 take into account other factors such as density, thickness of the material as well as factors  
129 relating to the type of building and the intended use of the material (bulk or superficial)*". The  
130 current study implements improvements, based on scientific data available in literature, into  
131 the existing and validated Markkanen room model. A sensitivity analysis of the different  
132 parameters impacting the calculated absorbed dose rate in air is performed. For the different  
133 improvements implemented in the dosimetric evaluation the impact and practicality for  
134 industrial implementation is discussed.

## 135 136 **2. Materials & Methods**

### 137 138 **2.1 Materials**

139

140 For the evaluation of the dose model the composition of concrete, defined by NIST [32], is  
 141 used, except when mentioned differently.

142

## 143 **2.2 Model**

144

### 145 **2.2.1 Model description**

146

147 To assess the absorbed dose rate in air ( $D_A$ ), the room model of Markkanen [1] (see Equation  
 148 1) is used.

149

150

$$151 \quad D_A = 5.77 \times 10^{-7} \frac{AC\rho}{4\pi} \sum \gamma_i \left( \frac{\mu_{en}}{\rho} \right)_i E_i \int B_i \frac{e^{-\mu_i s}}{l^2} dV \quad (1)$$

152

153

154 With  $D_A$  the absorbed dose rate in air in Gy/h,  $AC$  the activity concentration of a radionuclide  
 155 incorporated in the material of concern in Bq/kg,  $\rho$  the density of the material in kg/m<sup>3</sup>,  $\gamma_i$  the  
 156 gamma intensity of gamma line  $i$ ,  $(\mu_{en}/\rho)_i$  the energy absorption coefficient in air for gamma  
 157 energy  $E_i$  in cm<sup>2</sup>/g,  $E_i$  the photon energy in MeV,  $\mu_i$  the linear attenuation coefficient of the  
 158 material for gamma energy  $E_i$  in cm<sup>-1</sup>,  $B_i$  the dose build up factor (see Equation 2) calculated  
 159 via the Berger's formula,  $l$  the distance between the point of detection ( $x_p, y_p, z_p$ ) and the point  
 160 of integration in cm (see Equation 4) and  $s$  the fraction of  $l$  within the top layer in cm (see  
 161 Equation 3). The total exposure rate is the sum of the exposure rates calculated from ceiling,  
 162 floor and each wall. The  $(\mu_{en}/\rho)_i$  is a polynomial best fit achieved from the data reported by  
 163 Martin [33] using the data of Hubbell and Seltzer [34].

164

$$165 \quad B_i = 1 + C(E_i)\mu_i s e^{D(E_i)\mu_i s} \quad (2)$$

166

167 In literature different  $C$  and  $D$  parameters are proposed by different authors. In the model  
 168 described here, the values of  $C$  and  $D$  proposed by Pelliccioni [35] are used. These are  
 169 calculated for the energy spectrum via logarithmic and exponential best-fit function  
 170 respectively by using the concrete parameters described by Pelliccioni [35] at 7 mean free  
 171 paths (mfp).

172

$$173 \quad s = \left| \frac{z}{z_p - z} \right| l \quad (3)$$

174

$$175 \quad l = \sqrt{(x_p - x)^2 + (y_p - y)^2 + (z_p - z)^2} \quad (4)$$

176

177 In order to convert the  $D_A$  to effective dose a conversion factor of 0.7 Sv/Gy is used [28]. This  
 178 conversion factor is used for all gamma emitters and originates from the UNSCEAR 2000 report  
 179 [3].—This conversion factor is used in the dose calculations considered in this article and is  
 180 consequently used for comparison reasons. Nevertheless, nuclide specific conversion factors  
 181 have been suggested by Krstic and Nikezic [36].

182

183 The model assumes a homogeneous sample composition and a homogeneous distribution of  
184 the radionuclides throughout the composed materials. In addition a standard room is used as  
185 a reference throughout the paper. The standard room size was described by Koblinger [15] as  
186 measuring 400 cm x 500 cm x 280 cm. Here a standard thickness of walls, floor and ceiling of  
187 20 cm is assumed. Neither doors nor windows are present and the point of detection ( $x_p$ ,  $y_p$ ,  
188  $z_p$ ) is set at the middle of the room. Whereas Koblinger suggested a density of 2320 kg/m<sup>3</sup>, RP-  
189 112 suggests a density of 2350 kg/m<sup>3</sup> [15,28]. The value of 2350 kg/m<sup>3</sup> is used here as a  
190 standard.

191 No background correction is assumed when calculating the  $D_A$ .

192

193 All calculations are performed by a combination of Microsoft® excel and R® [37]. The input  
194 parameters are submitted in Microsoft® excel whereas the further treatment of the input data  
195 is performed by Microsoft® excel and R®.

196

### 197 2.2.2. Selection of the number of gamma lines

198

199 In order to check the impact of the number of gamma lines, a comparison of the absorbed  
200 dose rate in air is made between different dose assessment models for a standard room. The  
201 Markkanen [1], Mustonen [22], ISS room model [23] and the model developed in this study,  
202 further called Expanded Gamma Dose Assessment (EGDA) model, are compared. Different  
203 versions of the EGDA model are evaluated depending on the number of gamma lines used for  
204 the dose assessment. 'EGDA>1%', 'EGDA>0.1%', 'EGDA>0%' take into account all gamma lines  
205 which have a gamma emission intensity (including the branching factor) above respectively 1  
206 %, 0.1 % and 0 % when considering gamma emission lines from the <sup>238</sup>U, <sup>232</sup>Th and <sup>235</sup>U decay  
207 series and <sup>40</sup>K. In addition two variants of 'EGDA>0.1%' are discussed. In one variant the  
208 emission gamma lines of <sup>238</sup>U and <sup>232</sup>Th (except for the 2614 keV gamma emission line since  
209 this emission line represents over 40 % of the dose rate of the <sup>232</sup>Th decay series) of  
210 'EGDA>0.1%' are converted to one weighted average gamma emission line. This variant is  
211 indicated in Table 1 by the suffix "averaged". In the second variant the emission gamma lines  
212 which have a gamma emission intensity lower than 0.1 % are converted to one weighted  
213 average gamma line for <sup>238</sup>U, <sup>232</sup>Th and <sup>235</sup>U. This variant is indicated in Table 1 as "EGDA+".  
214 Details on each model are provided in Table 1. Since not all the details necessary for the  
215 calculations were present in the original paper of Markkanen [1] and Mustonen [22], updated  
216 values were used (details in Table 1). This is indicated by a suffix "updated". In addition, a  
217 second variant of the ISS room model, which makes use of the Berger parameters described  
218 by Pelliccioni [35] instead of the Berger parameters of Markkanen [1], is discussed. This variant  
219 is indicated with the infix "Pelliccioni" whereas the original ISS room model is indicated with  
220 the infix "original". For readability, abbreviations of the dose model names are provided in  
221 Table 1 and Table 5.

222

223 Table 1: Overview of the different dose calculation models and their parameters used to  
 224 evaluate the absorbed dose rate in air.

Model	Markkanen original	Markkanen updated	Mustonen updated	ISS original room model	ISS Pelliccioni room model	EGDA>1%	EGDA>0.1%	EGDA>0.1% averaged	EGDA+	EGDA>0%
<b>Concrete composition</b>	Markkanen 1995 [1]	Ordinary Portland concrete (NIST)	Ordinary Portland concrete (NIST)	Ordinary Portland concrete (NIST)	Ordinary Portland concrete (NIST)	Ordinary Portland concrete (NIST)	Ordinary Portland concrete (NIST)	Ordinary Portland concrete (NIST)	Ordinary Portland concrete (NIST)	Ordinary Portland concrete (NIST)
<b>Energy absorption coefficient in air</b>	Markkanen 1995 [1]	Best fit from Martin 2006 [33]	Best fit from Martin 2006 [33]	Hubbell 1982 [38]	Hubell 1982 [38]	Best fit from Martin 2006 [33]				
<b>Density (kg/m<sup>3</sup>)</b>	2350	2350	2350	2350	2350	2350	2350	2350	2350	2350
<b>Linear attenuation coefficient</b>	From Markkanen 1995 [1]	XCOM [39]: ordinary Portland concrete (NIST)	XCOM [39]: ordinary Portland concrete (NIST)	Hubbell 1982 [38]	Hubbell 1982 [38]	XCOM [39]: ordinary Portland concrete (NIST) or IP	XCOM [39]: ordinary Portland concrete (NIST) or IP	XCOM [39]: ordinary Portland concrete (NIST) or IP	XCOM [39]: ordinary Portland concrete (NIST) or IP	XCOM [39]: ordinary Portland concrete (NIST) or IP
<b>Gamma emission energy and intensity</b>	Markkanen 1995 [1]	Mustonen 1984 [22]	Mustonen 1984 [22]	NuDat website [40]	NuDat website [40]	DDEP website [31]				
<b>Berger Parameters</b>	Markkanen 1995 [1]	Best fit of Pelliccioni 1989 [35]	Best fit of Pelliccioni 1989 [35]	Best fit of Markkanen 1995 [1]	Best fit of Pelliccioni 1989 [35]	Best fit of Pelliccioni 1989 [35]	Best fit of Pelliccioni 1989 [35]	Best fit of Pelliccioni 1989 [35]	Best fit of Pelliccioni 1989 [35]	Best fit of Pelliccioni 1989 [35]
<b>Number of gamma lines <sup>238</sup>U</b>	1	1	24	19*	19*	82	87	1*	87 + 1**	761
<b>Gamma emission intensity <sup>238</sup>U***</b>	2.12	2.12	2.12	2.41	2.41	2.19	2.36	2.36	2.41	2.41
<b>Number of gamma lines <sup>232</sup>Th</b>	2	2	20	14*	14*	36	110	2*	110 + 1**	349

<b>Gamma emission intensity <sup>232</sup>Th***</b>	2.41	2.41	2.41	2.63	2.63	2.76	2.98	2.98	3.04	3.04
<b>Number of gamma lines <sup>40</sup>K</b>	1	1	1	1	1	1	1	1	1	1
<b>Gamma emission intensity <sup>40</sup>K</b>	0.107	0.107	0.107	0.107	0.107	0.1055	0.1055	0.1055	0.1055	0.1055
<b>Number of gamma lines <sup>235</sup>U</b>	-	-	-	-	-	47	128	1*	128 + 1**	734
<b>Gamma emission intensity <sup>235</sup>U***</b>	-	-	-	-	-	2.78	3.04	3.04	3.1	3.1
<b>Model abbreviation</b>	Mark <sub>orig</sub>	Mark <sub>upd</sub>	Must <sub>upd</sub>	ISS <sub>orig</sub>	ISS <sub>Pelli</sub>	-	-	-	-	-

\* 87, 109 and 128 gamma emission lines are converted to 1 for respectively <sup>238</sup>U, <sup>232</sup>Th and <sup>235</sup>U

\*\* 674, 239 and 606 gamma emission lines are converted to 1 for respectively <sup>238</sup>U, <sup>232</sup>Th and <sup>235</sup>U

\*\*\* The gamma emission intensity is the sum of the individual gamma-ray emission energies.

225

### 226 2.2.3. Role of the build-up factor

227

228 The impact of the build-up factor (B) was evaluated for a standard room by using different  
 229 sets of Berger parameters C and D to calculate the D<sub>A</sub> per unit of activity concentration. The  
 230 Berger parameters as described by Markkanen and by Pelliccioni were compared [1,35]. In  
 231 addition the case without Berger parameters (C=D=0) is evaluated, meaning the role of build-  
 232 up factor is neglected. The latter case is indicated by the suffix "B = 1" in Table 4.

233

### 234 2.2.4. Role of the presence disequilibria in the <sup>232</sup>Th, <sup>238</sup>U and <sup>235</sup>U decay series

235

236 For model 'EGDA>0.1%' the contribution of long living radionuclides and their progeny to the  
 237 total absorbed dose rate in air per unit of activity concentration for the decay series of <sup>238</sup>U  
 238 and <sup>232</sup>Th is evaluated. The <sup>238</sup>U decay chain is divided into 3 subchains : i.e. <sup>238</sup>U-part (<sup>238</sup>U to  
 239 <sup>230</sup>Th), <sup>226</sup>Ra-part (<sup>226</sup>Ra to <sup>214</sup>Po) and <sup>210</sup>Pb-part (<sup>210</sup>Pb to <sup>210</sup>Po). Similar, the <sup>232</sup>Th decay chain  
 240 is divided into <sup>232</sup>Th-part (only <sup>232</sup>Th), <sup>228</sup>Ra-part (<sup>228</sup>Ra to <sup>228</sup>Ac) and <sup>228</sup>Th-part (<sup>228</sup>Th to <sup>208</sup>Tl).  
 241 The absorbed dose rate in air of <sup>235</sup>U is evaluated in the framework of the ratio of AC of  
 242 <sup>238</sup>U/<sup>235</sup>U i.e. 21.6 as expected value for non- diluted/enriched samples. No disequilibrium is

243 considered in case of  $^{235}\text{U}$  decay series as (dis)equilibrium in this decay series is often not  
244 reported.

245

#### 246 2.2.5 Impact of sample specific composition

247

248 The impact of the sample composition on the dose rate is compared by simulating a room  
249 constructed out of Fayalite Slag based Inorganic Polymers (FSIPs). FSIPs have different  
250 chemical, physical and structural properties than concrete. The characteristics of FSIPs are  
251 described by Kriskova et al. [41], Onisei et al. [42] and Iacobescu et al. [43]. The sample  
252 composition differs from concrete consequently leading to the usage of different linear  
253 attenuation coefficients. The attenuation coefficients are calculated for each gamma emission  
254 energy via the XCOM program [44]. The sample specific coherent mass attenuation coefficient  
255 of XCOM is therefore converted to the sample specific linear attenuation coefficient.

256

### 257 **2.3. Sensitivity Analysis**

258

259 A sensitivity analysis of the parameters impacting the absorbed dose rate in air is performed.  
260 The studied parameters are density, wall thickness, presence of windows and doors and room  
261 size. All parameters are compared to the standard parameters of a standard concrete room  
262 as defined in section 2.2.1.

263

#### 264 2.3.1. Density

265

266 The impact of the wall density on the  $D_A$  is tested for a standard room with density varying  
267 stepwise (step size of  $100 \text{ kg/m}^3$ ) between  $1000 \text{ kg/m}^3$  and  $3500 \text{ kg/m}^3$ , corresponding to the  
268 density of hollow bricks up to the density of high density concrete.

269

#### 270 2.3.2. Wall Thickness

271

272 In a standard concrete room the wall thickness is assumed to be 20 cm. However depending  
273 on the usage thinner or thicker walls are required. The impact of the wall thickness on the  $D_A$   
274 in the standard room is tested with wall thickness varying stepwise (step size of 5 cm) between  
275 5 cm and 80 cm while keeping floor and ceiling thickness constant at 20 cm.

276

#### 277 2.3.3. Room Size

278

279 The impact of the room size on the  $D_A$  is tested for a concrete room. A square room is  
280 simulated with length of the wall varying stepwise (step size of 100 cm) between 100 cm and  
281 1000 cm for a room height of 280 cm and between 100 cm and 1183.2 cm for a room height  
282 of 200 cm.

283

#### 284 2.3.4 Presence of windows and doors

285

286 The EU-BSS assumes a standard room without the presence of windows and doors. This is a  
287 strict approach but not realistic. The impact of the presence of windows or doors of different  
288 surfaces is tested. Tests are conducted for surfaces of  $1 \text{ m}^2$ ,  $2 \text{ m}^2$  and  $4 \text{ m}^2$  positioned in the

289 middle or the corner of a wall or ceiling. The imaginary dose rate originating of the specific  
 290 window/door surface is subtracted from the dose rate of the wall without any window/door.

291

292 **2.4 Comparison of index and dose assessment tools**

293

294 A comparison is made of the most used index and dose calculations relevant for the dose  
 295 assessment within the European legislative framework applicable towards building materials.  
 296 More details regarding these different index and dose calculations are shown in Table 2 or can  
 297 be found in the respective references.

298

299 The index values calculated via ACI and the density and thickness corrected index (I(pd)) are  
 300 compared using the AC of different types of residues and cement shown in Table 3 [1,2,4]. The  
 301 obtained dose of the Markkanen original, density and thickness corrected (D(pd)) and  
 302 EGDA>0% dose calculations are compared using the same AC [1,2,30]. In addition to the  
 303 standard density of 2350 kg/m<sup>3</sup> and standard thickness of 20 cm, six different scenarios are  
 304 tested with varying density and thickness (Table 4). In the comparisons, it is assumed that the  
 305 residues are solely used to construct a building material, this because recent studies [45,46]  
 306 indicate the applicability of building materials without the use of any additives like cement,  
 307 sand, gravel, etc. The AC values originate from Nuccetelli et al. [10]. In all cases the exposure  
 308 time is 7000 h.

309

310 Table 2: Overview of the parameters of the index and dose calculations used in the European  
 311 legislative framework applicable towards building materials.

	Index calculation		Dose calculation		
	ACI	I(pd)	Markkanen original	D(pd)	EGDA>0%
<b>Geometry</b>	Floor, ceiling, 4 walls	Floor, ceiling, 4 walls	Floor, ceiling, 4 walls	Floor, ceiling, 4 walls	Floor, ceiling, 4 walls
<b>Size geometry (cm<sup>3</sup>)</b>	400 x 500 x 280*	400 x 500 x 280	400 x 500 x 280	400 x 500 x 280	(Flexible) Here 400 x 500 x 280
<b>Wall thickness (cm)</b>	20	Flexible	20	Flexible	Flexible
<b>Density (kg/m<sup>3</sup>)</b>	2350**	Flexible	2350**	Flexible	Flexible
<b>Background correction</b>	70 nGy/h	50 nGy/h	0.348 mSv	0.245 mSv	0.245 mSv

<b>Composition</b>	Concrete	Concrete	Concrete	Concrete	(Flexible) Here Concrete
<b>Reference(s)</b>	EC 2014; RP112; Markkanen 1995	Nucetelli et al. 2015	EC 2014; RP112; Markkanen 1995	Nucetelli et al. 2015	

\* In Markkanen 1995 size is 12 x 7 x 2.8 m<sup>3</sup> with thickness of 0.2 m

\*\* In Markkanen 1995 density is 2320 kg/m<sup>3</sup>

312

313 Table 3: Activity concentrations (Bq/kg) of <sup>226</sup>Ra, <sup>232</sup>Th and <sup>40</sup>K present in different residues

314 and cement.

<b>Material type</b>	<b><sup>226</sup>Ra (Bq/kg)</b>	<b><sup>232</sup>Th (Bq/kg)</b>	<b><sup>40</sup>K (Bq/kg)</b>	<b>Reference</b>
<b>Furnace slags *</b>	147	42	258	Nucetelli et al. 2015
<b>Bottom ash and fly ash *</b>	207	80	546	Nucetelli et al. 2015
<b>Phosphogypsum *</b>	381	22	71	Nucetelli et al. 2015
<b>Bauxite residue *</b>	337	480	205	Nucetelli et al. 2015
<b>Cement *</b>	42	32	214	Nucetelli et al. 2015

315

\* Average values of database from Nucetelli et al. 2015 [10]

316

317 Table 4: Description of 6 different scenarios which are described by a specific set of density

318 and thickness. The scenarios are used for the comparison of the models of Table 2.

319

<b>Scenario number</b>	1	2	3	4	5	6
<b>Thickness (cm)</b>	10	10	18	25	40	40
<b>Density (kg/m<sup>3</sup>)</b>	1400	3000	3000	1400	1400	3000

320

321

### 322 **3. Results and discussion**

323

324 In section 3.1 the different absorbed dose rates in air per unit of activity concentration for  
325 <sup>238</sup>U, <sup>232</sup>Th, <sup>40</sup>K and <sup>235</sup>U obtained by different dose assessment models are compared. This  
326 section discusses the impact of working with averaged gamma emission lines as well as the  
327 impact of the build-up factor and the radiological equilibria.

328

329 Based on this comparison, the most practical EGDA model with the highest gamma emission  
330 intensity is selected and in section 3.2 a sensitivity analysis of this model is performed by  
331 changing wall thickness and density, room size and the presence of windows and doors.  
332 Throughout section 3.1 and 3.2 the impact of the sample composition is quantified.

333

334 Section 3.3 deals with the application of the model focussing on the dosimetric evaluation,  
335 the impact and the practicality for industrial implementation. Consequently a comparison is

336 performed of the most used index and dose calculations relevant for the dose assessment  
 337 within the European legislative framework applicable towards building materials.

338

339 **3.1. Model**

340

341 **3.1.1. Impact of the number of gamma lines**

342

343 Table 5 shows the  $D_A$  per unit of activity concentration for  $^{238}\text{U}$ ,  $^{232}\text{Th}$ ,  $^{40}\text{K}$  and  $^{235}\text{U}$  of the  
 344 different models described in Table 1. The different models assume a concrete standard room  
 345 unless indicated else by suffix FSIP.

346

347 Table 5: Overview of the absorbed dose rate in air per unit of activity concentration (nGy/h  
 348 per Bq/kg) for  $^{238}\text{U}$ ,  $^{232}\text{Th}$ ,  $^{40}\text{K}$  and  $^{235}\text{U}$  calculated by different dose assessment calculation  
 349 models described in Table 1.

350

	$^{238}\text{U}$	$^{232}\text{Th}$	$^{40}\text{K}$	$^{235}\text{U}$
<b>Model abbreviation</b>	<b>Dose rate in air (<math>D_A</math>) (nGy/h per Bq/kg)</b>	<b>Dose rate in air (<math>D_A</math>) (nGy/h per Bq/kg)</b>	<b>Dose rate in air (<math>D_A</math>) (nGy/h per Bq/kg)</b>	<b>Dose rate in air (<math>D_A</math>) (nGy/h per Bq/kg)</b>
Mark <sub>orig</sub>	0.908	1.06	0.0767	-
Mark <sub>orig B=1</sub>	0.3845	0.5	0.0408	-
Mark <sub>upd</sub>	0.893	1.02	0.0778	-
Mark <sub>upd B=1</sub>	0.383	0.501	0.0407	-
Must <sub>upd</sub>	0.84	0.999	0.0778	-
Must <sub>upd B=1</sub>	0.0405	0.51	0.0407	-
ISS <sub>orig</sub>	0.894	1.138	0.0767	-
ISS <sub>Pelli</sub>	0.869	1.109	0.0767	-
EGDA>1%	0.76	0.967	0.0767	0.228
EGDA>0.1%	0.826	1.06	0.0767	0.25
EGDA>0.1% <sub>B=1</sub>	0.395	0.535	0.0401	0.0819
EGDA>0.1% FSIP	0.838	1.07	0.0784	0.234
EGDA>0.1% <sub>aver</sub>	0.88	1.07	0.0767	0.239
EGDA>0.1% <sub>aver B=1</sub>	0.368	0.51	0.0401	0.0725
EGDA+	0.85	1.08	0.0767	0.255
EGDA>0%	0.849	1.08	0.0767	0.256

351 Suffix 'orig' (original): Data of the original paper are used as shown in Table 2.

352 Suffix 'upd' (updated): Updated data, as shown in Table 2, are used with the original calculation method.

353 Suffix 'B=1' (build-up factor = 1): The Berger parameters are set to zero. This means the role of the build-up  
 354 factor is negligible.

355 Suffix 'aver' (averaged): Several gamma lines are reduced to a single weighted average gamma emission line.

356 Suffix 'Pelli' (Pelliccioni): the Berger parameters as described by Pelliccioni 1989 are used.

357 FSIP: The chemical composition of the room components is set to the FSIP chemical composition.

358

359 Comparing the  $D_A$  between  $Mark_{orig}$  and  $Mark_{upd}$ , an increase of 1.7 % and 3.8 % is observed  
360 for respectively  $^{238}U$  and  $^{232}Th$ , in favour of the  $Mark_{orig}$  model. In case of  $^{40}K$  a decrease of 1.4  
361 % is observed in favour of the  $Mark_{orig}$  model. This deviation in  $D_A$  is due to the usage of  
362 different Berger parameters and a different concrete composition in the two models (Table  
363 1).

364  
365 The 24 emission gamma lines of  $^{238}U$  and the 19 gamma emission lines (2614 keV-line is  
366 excluded) of  $^{232}Th$  of the Mustonen model are converted to a single weighted average gamma  
367 emission line for  $^{238}U$  and  $^{232}Th$  in the Markkanen model.

368 Comparing  $Mark_{upd}$  with  $Must_{upd}$  a 6 % and 2 % increase in  $D_A$  is observed for respectively  $^{238}U$   
369 and  $^{232}Th$ . This increase is solely due to usage of averaged gamma lines in the Markkanen  
370 model. In case of  $^{235}U$  a decrease in the  $D_A$  of 4.6 % (4.9 %) is observed for the 'averaged EGDA'  
371 variant. The differences are solely due to the usage of energy specific attenuation coefficients  
372 and energy specific C and D Berger parameters as the total gamma intensity stays equal.

373  
374 When comparing the EGDA models with  $Mark_{upd}$ ,  $Must_{upd}$  and the ISS room models one can  
375 see that the number of gamma lines used is much higher (Table 1). When more gamma lines  
376 are included in the EGDA model the gamma emission intensity also increases for  $^{238}U$ ,  $^{232}Th$   
377 and  $^{235}U$ , leading to higher  $D_A$  when comparing EGDA>1%, EGDA>0.1% and EGDA>0%.  
378 However the gamma emission intensity of the ISS room model is smaller than the gamma  
379 emission intensity of EGDA>0% for  $^{238}U$  and  $^{232}Th$  (Table 1), still the  $D_A$  of the ISS room model  
380 is higher than the  $D_A$  of EGDA>0% (Table 5). The usage of a set of averaged gamma-lines in the  
381 ISS room models tends to increase the  $D_A$ , as discussed above. In addition the usage of other  
382 B in the  $ISS_{orig}$  (Table 1) also impacts the  $D_A$ , this is discussed in section 3.1.2.

383  
384 The EGDA>0% model uses all the gamma lines available originating from  $^{238}U$ ,  $^{232}Th$ ,  $^{235}U$  and  
385  $^{40}K$ . In total 1845 gamma lines are used in the calculation by model EGDA>0% whereas in  
386 model EGDA>0.1% 326 gamma lines are used. The gamma emission intensity of EGDA>0.1%  
387 is 2.1 %, 2.0 % and 1.9 % lower than EGDA>0% for respectively  $^{238}U$ ,  $^{232}Th$  and  $^{235}U$ .  
388 Nevertheless, when using a higher number of gamma lines also the calculation time increases.  
389 In order to limit the calculation but still consider the maximum gamma emission intensity, the  
390 extra gamma lines of EGDA>0% in comparison to EGDA>0.1% are converted to 3 weighted  
391 average gamma lines; one line for  $^{238}U$ ,  $^{232}Th$  and  $^{235}U$ . This approach is incorporated in the  
392 EGDA+ model (Table 1). The difference in  $D_A$  between EGDA+ and EGDA>0% is limited to plus  
393 0.001 nGy/h per Bq/kg for  $^{238}U$  and minus 0.001 nGy/h per Bq/kg for  $^{235}U$ . In case of  $^{232}Th$  no  
394 difference was observed.

395

### 396 3.1.2. Impact of the Build-up factor

397

398 Table 5 shows the  $D_A$  for several models. Comparing the  $D_A$  of the "B=1" variants with the non-  
399 unity originals, a significant decreases in the  $D_A$  is present. For example in the case of  
400 EGDA>0.1% the "B=1" variant has an  $D_A$  which is approximately 52 %, 50 %, 48 % and 67 %  
401 lower for respectively  $^{238}U$ ,  $^{232}Th$ ,  $^{40}K$  and  $^{235}U$ . The presence of the B is consequently  
402 important when calculating the  $D_A$ . The  $ISS_{Pelli}$  model differs only from the  $ISS_{orig}$  model by the  
403 usage of the data of Pelliccioni instead of the data of Markkanen to calculate the B. Comparing  
404 both models, the  $D_A$  per unit of activity concentration of the  $ISS_{Pelli}$  model is 2.8 % and 2.6 %  
405 lower for respectively  $^{238}U$  and  $^{232}Th$  in case of a standard concrete room.

406  
407  
408  
409  
410  
411  
412

### 3.1.3. Impact of disequilibrium in the $^{232}\text{Th}$ , $^{238}\text{U}$ and $^{235}\text{U}$ decay series

Table 6: Absorbed dose rate in air ( $D_A$ ) per unit of activity concentration (nGy/h per Bq/kg) of the long-living radionuclides and their progeny of the  $^{238}\text{U}$  and  $^{232}\text{Th}$  decay series in case of the EGDA>0.1% model.

Concrete standard room					
$^{238}\text{U}$ Decay series			$^{232}\text{Th}$ Decay series		
	$D_A$ (nGy/h per Bq/kg)	% Contribution		$D_A$ (nGy/h per Bq/kg)	% Contribution
$^{238}\text{U}$ Part	0.0077	0.931	$^{232}\text{Th}$ Part	0.000041	0.004
$^{226}\text{Ra}$ Part	0.82	99.002	$^{228}\text{Ra}$ Part	0.42	39.583
$^{210}\text{Pb}$ Part	0.00055	0.067	$^{228}\text{Th}$ Part	0.64	60.413

413  
414  
415  
416  
417  
418  
419  
420  
421  
422  
423  
424  
425  
426  
427  
428  
429  
430  
431  
432  
433  
434  
435

Considering the decay series of  $^{238}\text{U}$ : the  $^{238}\text{U}$ -part,  $^{226}\text{Ra}$ -part and  $^{210}\text{Pb}$ -part of the decay chain represent respectively approximately 0.93 %, 99 % and 0.067 % of the total external absorbed gamma dose rate in air per unit of activity concentration of the whole  $^{238}\text{U}$  decay series, in the case of a standard concrete room. The lifespan of a building material will not allow reestablishing the equilibrium between the  $^{238}\text{U}$ -part and  $^{226}\text{Ra}$ -part. Looking solely at the lifespan aspect, it would be meaningful to treat both parts of the decay chain separately. However, this is not always feasible since one must be able to measure  $^{238}\text{U}$ ,  $^{234}\text{Th}$  or  $^{234}\text{Pa}$ . Using in this case the AC of  $^{226}\text{Ra}$  for the whole decay series will only introduce a small bias since  $^{238}\text{U}$  part and  $^{210}\text{Pb}$  contribute less than 1 % to the total  $D_A$  of the  $^{238}\text{U}$  decay series. On the other hand using the AC of  $^{238}\text{U}$  for  $^{226}\text{Ra}$  and its decay products would have a large impact as  $^{226}\text{Ra}$ -part represents 99 % of the  $D_A$  of the  $^{238}\text{U}$  decay series. The suggestion of RP-122 to use the highest AC present in the decay series would overestimate the gamma dose rate when the AC of  $^{238}\text{U}$  or  $^{210}\text{Pb}$  is larger than the AC of  $^{226}\text{Ra}$ . Due to the small contribution of  $^{210}\text{Pb}$ -part to the gamma dose (i.e. 0.067%), the activity concentration of  $^{226}\text{Ra}$  is used for the  $^{210}\text{Pb}$ -part of the decay series in this study. The half-life of  $^{222}\text{Rn}$  allows radon exhalation from the building material which decreases the external absorbed gamma dose rate in air. De Jong and Van Dijck (2008) [18] showed that the external absorbed gamma dose rate in air decreased on average with 9 % and 5 % for respectively gypsum and concrete used in the Netherlands. In addition the EU-BSS [4] treats the radon exposure (from soil and building materials) separately from the gamma exposure linked to building materials. For this reason all the EGDA models do not consider radon and is therefore stricter in terms of gamma ray exposure.

436  
437  
438  
439  
440  
441  
442  
443  
444  
445

Considering the decay series of  $^{232}\text{Th}$ : the  $^{232}\text{Th}$ -part,  $^{228}\text{Ra}$ -part and  $^{228}\text{Th}$ -part of the decay chain represent respectively approximately 0.004 %, 39.6 % and 60.4 % (Table 6) of the total external absorbed gamma dose rate in air per unit of activity concentration of the whole  $^{232}\text{Th}$  decay series in the case of a standard concrete room. Disequilibria in the  $^{232}\text{Th}$  decay chain are complex and insights in the production process of NORM-residues can provide useful information. In the case of complete Th-separation, the equilibrium will install within a timeframe of 40 years in the Th-bearing residue. Whereas in the Ra-bearing residue the activity will fade away. The lifetime of building materials can be considered to cover this timespan. Being strict, it is best not to consider disequilibrium and consider the highest activity concentration that is possible and use for the complete (so 100 %)  $D_A$  calculation of the  $^{232}\text{Th}$

446 decay series. An adequate determination of the activity concentration is recommended to  
447 assess whether or not disequilibria are present. In addition it is assumed in this study that no  
448  $^{220}\text{Rn}$  exhalation from the building material takes place as the half-life of  $^{220}\text{Rn}$  is relatively  
449 short (55.8 sec).

450

451 To the authors knowledge in none of current dose assessments tools available, the decay  
452 series of  $^{235}\text{U}$  is considered. However taking into account all the gamma emission intensities  
453 above 0.1 % the absorbed dose rate in air is 0.250 nGy/h per Bq/kg for a standard concrete  
454 room (Table 5). This is above the  $D_A$  of  $^{40}\text{K}$  on a Bq/kg level. However framing this  $^{235}\text{U}$   $D_A$  in a  
455 broader context, when the natural abundance of U is respected the AC of  $^{235}\text{U}$  is 0.0463 times  
456 the AC of  $^{238}\text{U}$ . So in reality the contribution of the  $D_A$  of  $^{235}\text{U}$  is of limited consequence, except  
457 when high activity concentrations of  $^{238}\text{U}$  are present. When no  $^{235}\text{U}$  is measured, the authors  
458 recommend using 0.0463 times the AC of  $^{238}\text{U}$  to implement the dose originating from  $^{235}\text{U}$ .  
459 Within the  $^{235}\text{U}$  decay series, disequilibrium situations can also be present but these are not  
460 considered here.

461

#### 462 3.1.4. Impact of sample specific composition

463

464 The impact of the sample composition is studied by comparing EGDA>0.1% and EGDA>0.1%  
465 FSIP. An increase in the  $D_A$  of 1.4 %, 0.9 % and 2.1 % is observed for  $^{238}\text{U}$ ,  $^{232}\text{Th}$  and  $^{40}\text{K}$  when  
466 FSIP is used instead of concrete. On the contrary, in case of  $^{235}\text{U}$ , a decrease in the  $D_A$  of 6.8 %  
467 is observed. It has to be noted that here solely the linear attenuation coefficients are changed.  
468 A change of sample composition implies also changing the energy and mfp-dependent B, due  
469 to the interdependency between the composition, the energy and the mfp. However, the  
470 study of this aspect is outside the scope of this paper.

471

#### 472 3.1.5. Selection of EGDA>0% model

473

474 The EGDA>0% model uses the highest gamma emission intensity and makes use of all the  
475 nuclear data on an individual base. Consequently this approach is the more accurate one and  
476 is selected for the performance of a sensitivity analysis in section 3.2. ~~The use of 3 weighted  
477 gamma emission lines in case of  $^{238}\text{U}$ ,  $^{232}\text{Th}$  and  $^{235}\text{U}$ , corresponding to respectively 2.1 %, 2.0  
478 % and 1.9 % of the total gamma emission intensity, allows performing faster calculations in  
479 comparison to EGDA>0% model.~~ The C and D Berger parameters described by Pelliccioni  
480 (1989) [35] are used for the calculations.

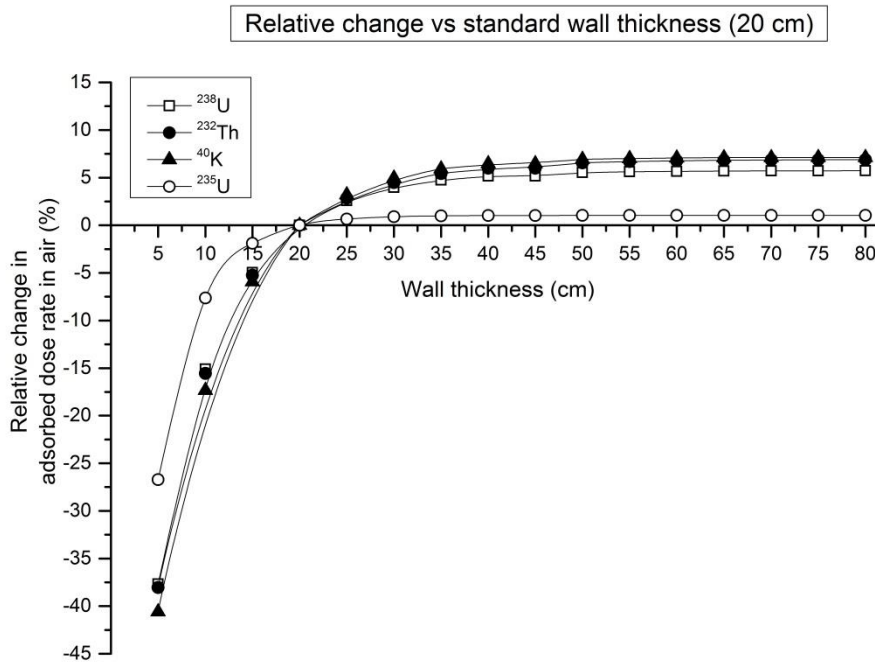
481 The presence of gamma emission by  $^{235}\text{U}$  is considered and disequilibrium situations can be  
482 considered when necessary.

483

### 484 **3.2. Sensitivity Analysis of EGDA>0% Model**

485

#### 486 3.2.1. Impact of the wall thickness calculated by the EGDA>0% model.



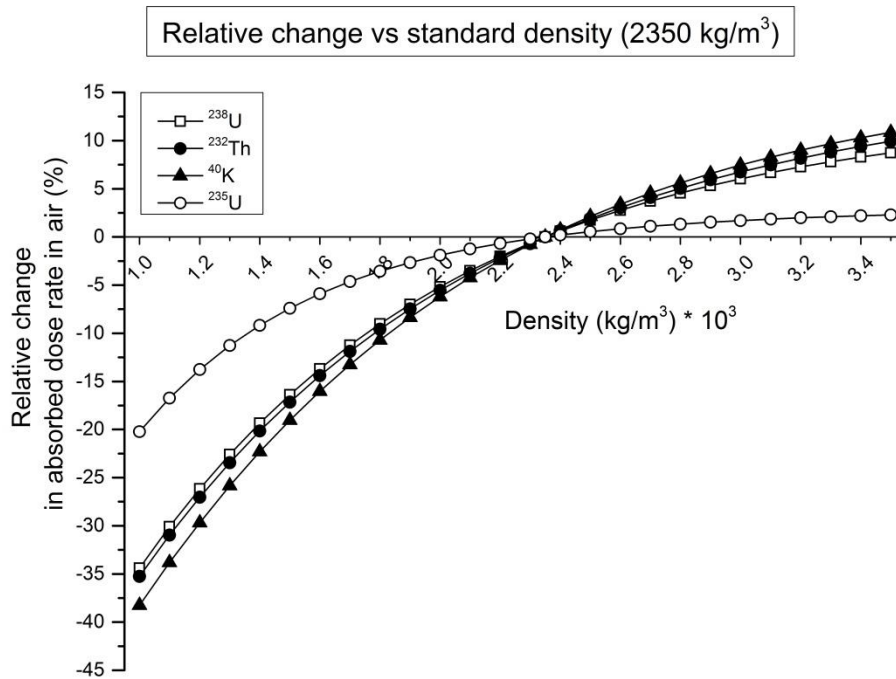
487  
 488 Figure 1: Relative change in the absorbed dose rate in air ( $D_A$ ) for a standard concrete room  
 489 with varying thickness (5-80 cm) vs a standard concrete room with wall thickness of 20 cm for  
 490  $^{238}\text{U}$ ,  $^{232}\text{Th}$ ,  $^{40}\text{K}$  and  $^{235}\text{U}$ . Relative change:  $(D_{A\text{thickness}_X} - D_{A\text{thickness}_{20\text{cm}}}) / (D_{A\text{thickness}_{20\text{cm}}} \times$   
 491 100)

492 Figure 1 shows the relative change (%) in  $D_A$  air for different thicknesses relative to the wall  
 493 thickness of 20 cm for  $^{238}\text{U}$ ,  $^{232}\text{Th}$ ,  $^{40}\text{K}$  and  $^{235}\text{U}$  in a standard concrete room. It is observed that  
 494 the relative decrease in  $D_A$  occurs rapidly with decreasing wall thickness. In case of a wall  
 495 thickness of 5 cm a relative decrease of 27.4 %, 27.6 %, 28.9 % and 21.1 % is observed for  
 496 respectively  $^{238}\text{U}$ ,  $^{232}\text{Th}$ ,  $^{40}\text{K}$  and  $^{235}\text{U}$ . In case of a wall thickness of 80cm a relative increase of  
 497 6.1 %, 7.4 %, 7.7 % and 1.1 % is observed for respectively  $^{238}\text{U}$ ,  $^{232}\text{Th}$ ,  $^{40}\text{K}$  and  $^{235}\text{U}$ . However, a  
 498 plateau in the increase of the  $D_A$  is observed. The percentage increase of the  $D_A$  between 20  
 499 cm and 25 cm thickness is below 1 % for  $^{235}\text{U}$  whereas for the other radionuclides this is  
 500 approximately 3 %. From a thickness of 40 cm, the increase in the  $D_A$  is below 1 % per increase  
 501 in 5 cm thickness for all the radionuclides. According to Risica et al. (2001) [27] this plateau  
 502 originates from self-absorption effects.

503  
 504 As the floor thickness is not varied the contribution of the walls to the  $D_A$  will increase with  
 505 the thickness. The contribution of the smaller wall (400 cm) will increase with approximately  
 506 5 % relative to the larger wall (500 cm) when increasing the wall thickness from 5 cm to 80  
 507 cm.

508  
 509 3.2.2. Impact of the density calculated by EGDA0% model

510  
 511



512  
513

514 Figure 2: Relative difference of the absorbed dose rate in air ( $D_A$ ) for a standard concrete room  
515 with varying density (1000-3500  $\text{kg/m}^3$ ) vs a standard concrete room with density of 2350  
516  $\text{kg/m}^3$  for  $^{238}\text{U}$ ,  $^{232}\text{Th}$ ,  $^{40}\text{K}$  and  $^{235}\text{U}$ . Relative change:  $(D_{A\text{density}_X} - D_{A\text{density}_{2350 \text{ kg/m}^3}}) /$   
517  $(D_{A\text{density}_{2350 \text{ kg/m}^3}} \times 100)$

518

519 Figure 2 shows the difference in  $D_A$  for different densities relative to the standard density of  
520  $2350 \text{ kg/m}^3$  for  $^{238}\text{U}$ ,  $^{232}\text{Th}$ ,  $^{40}\text{K}$  and  $^{235}\text{U}$  in a standard concrete room with thickness of 20 cm.  
521 At densities lower than  $2350 \text{ kg/m}^3$  a relative decrease in  $D_A$  is observed whereas a relative  
522 increase is observed at densities higher than  $2350 \text{ kg/m}^3$ . In case of a density of  $1000 \text{ kg/m}^3$   
523 a relative decrease of 34 %, 35 %, 38 % and 20 % is observed for respectively  $^{238}\text{U}$ ,  $^{232}\text{Th}$ ,  $^{40}\text{K}$  and  
524  $^{235}\text{U}$ . In case of a density of  $3500 \text{ kg/m}^3$  cm a relative increase of 9 %, 10 %, 11 % and 2 % is  
525 observed for respectively  $^{238}\text{U}$ ,  $^{232}\text{Th}$ ,  $^{40}\text{K}$  and  $^{235}\text{U}$ . With increasing densities the total number  
526 of radionuclides present in the material will increase leading to higher  $D_A$ . With decreasing  
527 densities to contrary is true.

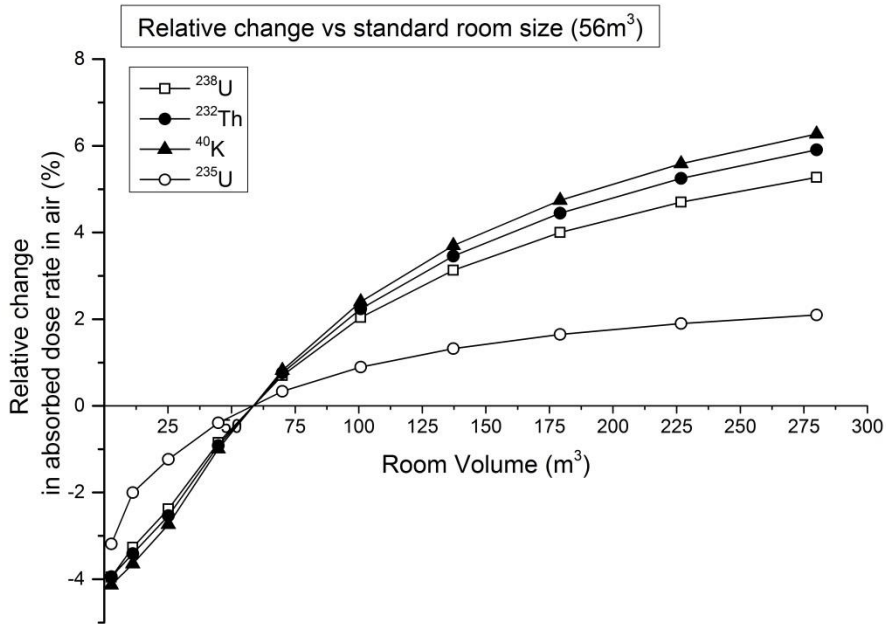
528

529 With increasing densities the relative contribution of the floor and ceiling to total dose rate  
530 decreases with approximately 1 % whereas the dose rate of the walls increases slightly. This  
531 effect is observed for the different radionuclides.

532

### 533 3.2.3. Impact of the room size calculated by the EGDA>0% model

534



535  
536

537 Figure 3: Relative difference of the absorbed dose rate in air for a standard concrete room  
538 with varying room size (2.8 - 280 m<sup>3</sup>) vs a standard concrete room with room size of 56 m<sup>3</sup> for  
539 <sup>238</sup>U, <sup>232</sup>Th, <sup>40</sup>K and <sup>235</sup>U.

540

541 Figure 3 shows the difference in D<sub>A</sub> for different room sizes relative to the standard room size  
542 (200 x 250 x 280 cm<sup>3</sup>) for <sup>238</sup>U, <sup>232</sup>Th, <sup>40</sup>K and <sup>235</sup>U in a standard concrete room. It is observed  
543 that the relative decrease in D<sub>A</sub> occurs with decreasing room size. In case of a room size of 2.8  
544 m<sup>3</sup> a relative decrease of 4 %, 4 %, 4 % and 3 % is observed for respectively <sup>238</sup>U, <sup>232</sup>Th, <sup>40</sup>K and  
545 <sup>235</sup>U. In case of a room size of 280 m<sup>3</sup> a relative increase of 5 %, 6 %, 6 % and 2 % is observed  
546 for respectively <sup>238</sup>U, <sup>232</sup>Th, <sup>40</sup>K and <sup>235</sup>U. With increasing room size to person standing in the  
547 room is surrounded by more material. Consequently the total number of radionuclides  
548 present in the room will also increase, leading to higher D<sub>A</sub>. With decreasing room size the  
549 contrary is true.

550 Figure 3 also shows that the influence of the room sizes affects the radionuclides differently.

551

552 Next to changing the room surface the impact of the room height is studied. At small room  
553 volumes (below approximately 15 m<sup>3</sup>), the D<sub>A</sub> of <sup>232</sup>Th is lower in case of a height of 200 cm  
554 than in case of a height of 280 cm. For a room area of 1 m<sup>2</sup> a difference of approximately 2.3  
555 %, 2.5 %, 2.7 % and 1.2 % difference for respectively <sup>238</sup>U, <sup>232</sup>Th, <sup>40</sup>K and <sup>235</sup>U is observed.  
556 However at room size larger than 15 m<sup>3</sup> the impact of height on the D<sub>A</sub> is reverted. At a room  
557 volume of 280 m<sup>3</sup> an increase in the D<sub>A</sub> of 1.7 %, 2.0 %, 2.1 % and 0.5 % for respectively <sup>238</sup>U,  
558 <sup>232</sup>Th, <sup>40</sup>K and <sup>235</sup>U is observed in favour of the room height of 200 cm .

559

560 3.2.4 The impact of the presence of windows and doors by the EGDA>0% model

561

562 Table 7: % Deviation in dose rate for different window surfaces located in the middle or the  
 563 corner of Wall 1 (400cmx280cm), Wall 2 (500x280cm) and the ceiling (400 cm x 500cm) in  
 564 comparison to respectively Wall 1, Wall 2 and the ceiling without the presence of windows.  
 565

	Window 100 cm x 100 cm		Window 100 cm x 200 cm		Window 200 cm x 200 cm	
	Middle	Corner	Middle	Corner	Middle	Corner
<b>% Deviation in absorbed dose rate in air (D<sub>A</sub>) originating from wall 1 (400 cm x 280 cm) with a window in comparison wall 1 without a window</b>						
<sup>238</sup> U	-11.8	-7.3	-22.5	-21.1	-43.2	-36.6
<sup>232</sup> Th	-11.8	-7.3	-22.5	-21.1	-43.1	-36.6
<sup>40</sup> K	-11.7	-7.4	-22.4	-21.0	-43.0	-36.6
<sup>235</sup> U	-12.1	-7.2	-23	-21.4	-43.9	-36.7
<b>% Deviation in absorbed dose rate in air (D<sub>A</sub>) originating from wall 2(500 cm x 280 cm) with a window in comparison to wall 2 without a window</b>						
<sup>238</sup> U	-11.7	-4.5	-21.9	-19.9	-41.1	-26.4
<sup>232</sup> Th	-11.6	-4.5	-21.8	-19.9	-41.0	-26.4
<sup>40</sup> K	-11.5	-4.6	-21.7	-19.8	-40.7	-26.4
<sup>235</sup> U	-12.2	-4.3	-22.6	-20.4	-42.2	-26.1
<b>% Deviation in absorbed dose rate in air (D<sub>A</sub>) originating from a ceiling (500 cm x 400 cm) with a window in comparison to a ceiling without a window</b>						
<sup>238</sup> U	-14.6	-2.2	-22.8	-6.4	-40.8	-17.3
<sup>232</sup> Th	-14.4	-2.3	-22.5	-6.4	-40.4	-17.2
<sup>40</sup> K	-13.9	-2.2	-21.7	-6.3	-39.2	-16.9
<sup>235</sup> U	-15.7	-2.1	-23.9	-6.1	-42.5	-16.9

566 Table 7 shows the percentage of deviation in the D<sub>A</sub> of the different room components in  
 567 comparison to the standard concrete room. With increasing size of the window or door  
 568 surface the D<sub>A</sub> of the component decreases. For example, in wall one the D<sub>A</sub> decreases with  
 569 approximately 12 % in case of a window of 100 cm x 100 cm whereas this decrease is  
 570 approximately 37 % for a window of 200 cm x 200 cm. In both cases the windows are  
 571 positioned in the middle of wall. Nevertheless the position of the surface in the component  
 572 plays an important role. In wall 2 the D<sub>A</sub> decreases for approximately 41% when the window  
 573 is positioned in the middle of the wall. When the same window is positioned in the corner, the  
 574 D<sub>A</sub> decreases with 26 % in comparison to a standard concrete room. In addition it must be  
 575 noted that in the case of a standard concrete room wall 1, wall 2 and the floor/ceiling  
 576 contribute for approximately 9.5 %, 14.5 % and 26 % respectively to the total D<sub>A</sub> of the room.  
 577 The final influence on the D<sub>A</sub> due to the presence of a window in the ceiling will be larger than  
 578 for a window in wall 1.  
 579

580  
 581 **3.3 Comparison of index and dose calculations**  
 582

583 Table 8: Overview of the index-values and effective dose (mSv/y) of the index and dose  
584 calculations used in the European legislative framework for different building materials  
585 consisting of residues or cement.  
586

	Index							
Model	ACI	I(pd)						
Thickness (cm)	20	10	10	18	20	25	40	40
Density (kg/m <sup>3</sup> )	2350	1400	3000	3000	2350	1400	1400	3000
Furnace slags	0.788	0.384	0.628	0.811	0.770	0.678	0.822	1.006
Bottom ash and fly ash	1.269	0.609	0.997	1.290	1.225	1.077	1.307	1.602
Phosphogypsum	1.405	0.719	1.171	1.510	1.434	1.264	1.529	1.864
Bauxite residue	3.592	1.657	2.710	3.509	3.330	2.928	3.554	4.355
Cement	0.385	0.180	0.295	0.382	0.363	0.319	0.387	0.476
Scenario number		1	2	3		4	5	6
	Dose (mSv/y)							
Model	Mark <sub>orig</sub>	D(pd)						
Thickness (cm)	20	10	10	18	20	25	40	40
Density (kg/m <sup>3</sup> )	2350	1400	3000	3000	2350	1400	1400	3000
Furnace slags	0.726	0.238	0.549	0.745	0.704	0.606	0.755	0.916
Bottom ash and fly ash	1.293	0.521	1.017	1.329	1.264	1.108	1.346	1.604
Phosphogypsum	1.592	0.659	1.237	1.595	1.521	1.342	1.614	1.905
Bauxite residue	3.825	1.841	3.190	4.043	3.865	3.437	4.087	4.796
Cement	0.206	-0.019	0.128	0.222	0.202	0.155	0.227	0.304
Scenario number		1	2	3		4	5	6
	Dose (mSv/y)							
Model	EGDA>0%							
Thickness (cm)		10	10	18	20	25	40	40
Density (kg/m <sup>3</sup> )		1400	3000	3000	2350	1400	1400	3000
Furnace slags		0.238	0.557	0.736	0.697	0.590	0.712	0.813
Bottom ash and fly ash		0.520	1.029	1.317	1.254	1.083	1.279	1.441
Phosphogypsum		0.661	1.252	1.577	1.506	1.313	1.533	1.710
Bauxite residue		1.830	3.192	3.971	3.798	3.337	3.868	4.323
Cement		-0.019	0.132	0.219	0.199	0.148	0.207	0.257
Scenario number		1	2	3		4	5	6

587  
588 Table 8 shows different index and dose values for 5 types of building materials calculated via  
589 different models described in Table 2. It must be noted that different authors and models use  
590 different background reductions like mentioned in Table 2. In addition in all calculations it is  
591 assumed that both the walls as the floor/ceiling have the same density and thickness. The ACI  
592 calculation is a non-flexible calculation and assumes a density of 2350 kg/m<sup>3</sup> and walls of 20  
593 cm thick and is considered as a reference for comparison since this is screening tool prescribed  
594 by the EU-BSS. Looking at a building material with density of 2350 kg/m<sup>3</sup> and thickness of 20

595 cm, the index value of the ACI is higher than the index value of I(pd) except for the  
596 phosphogypsum composition.

597 In case of building materials lighter than 2350 kg/m<sup>3</sup> and thinner than 20 cm building  
598 materials, the ACI overestimates the index-value in comparison to I(pd) (scenario 1). In  
599 scenario 2 and 3 the building material is thinner than 20cm and heavier than 2350 kg/m<sup>3</sup>. In  
600 scenario 2 solely overestimations by the ACI are observed. In scenario 3, an overestimation by  
601 the ACI only occurs in case of bauxite residue and cement. In contrast an underestimation  
602 occurs in case of furnace slags, bottom and fly ashes and phosphogypsum. In scenarios 4 and  
603 5 the building material is lighter than 2350 kg/m<sup>3</sup> and thicker than 20 cm. In scenario 4, the  
604 ACI overestimates the index value in comparison I(pd). In scenario 5 an overestimation by the  
605 ACI occurs in case of bauxite residue. In contrast an underestimation occurs in case of furnace  
606 slags, bottom and fly ashes, phosphogypsum and cement. Looking at building materials  
607 heavier than 2350 kg/m<sup>3</sup> and thicker than 20 cm, the ACI underestimates the index-value  
608 (scenario 6).

609  
610 In scenario 1 the ACI underestimates the index-value, it is recommended to use the I(pd) when  
611 that ACI index value is above 1. As in scenario 3 and 5 the ACI can over or underestimate the  
612 index value it is best to use the I(pd). As the density and thickness parameters of scenario 2  
613 and 4 correspond to the parameters of scenario 3 and 4 respectively, it is best to also use the  
614 I(pd) for scenario 2 and 4. For scenario 6 the ACI underestimates the index value and from a  
615 radioprotection point of view I(pd) is recommended.

616  
617 As underestimations by the Mark<sub>orig</sub> model (corresponds to ACI) in comparison to D(pd)  
618 (corresponds to I(pd)) occur in scenario 2, 3, 5 and 6, it is recommended from a  
619 radioprotection point of view to use the D(pd) calculation. In other scenarios it is  
620 recommended to use the D(pd) calculation when the effective dose approximates 1mSv/y.

621  
622 Comparing the D(pd) with EGDA>0% one can see that the D(pd)-dose-values are for all  
623 scenarios higher than the ones calculated via EGDA>0% except for scenario 1 and 2, which  
624 have a low wall thickness. In both scenarios, the EGDA>0% gives an effective dose which is  
625 solely a few μSv/y higher. In scenario 3, 4, 5 and 6 the EGDA>0% gives a dose which is from  
626 the order of 10 μSv/y to several 100's μSv/y lower. Therefore, in these scenarios, in case of an  
627 effective dose close to 1mSv calculated by D(pd), the authors recommend using a more  
628 detailed dose assessment model like EGDA>0% to more accurately assess the dose. It must  
629 also be noted that in this comparison the density and thickness of the walls and floor/ceiling  
630 are all equal. This can be different in reality and can affect the dose significantly. In addition  
631 one has to take into account that a room size larger than 400 cm x 500 cm x 280 cm gives rise  
632 to a dose increase like discussed in section 3.2.3. In addition, the presence of windows and  
633 doors will also impact this background correction as well as the different sample compositions.

634  
635 Regarding the different residues, the AC of a residue can vary according to the input, process  
636 parameters, etc. [47,48]. Therefore one cannot draw conclusions from the index and dose  
637 values of Table 8 on the usage of these classes of residues as building material but a case by  
638 case approach should be performed.

639  
640 **4. Conclusion**

641

642 The current study provides a dose calculation assessment based on the original dose  
643 calculation of Markkanen with expanded number of gamma lines and higher total gamma  
644 intensity. It is shown that working with averaged gamma lines increases the absorbed dose  
645 rate in air for  $^{238}\text{U}$  and  $^{232}\text{Th}$  with 6.1 % and 0.9 % respectively in case of a standard concrete  
646 room. In contrast, a decrease of 4.6 % is determined in case of  $^{235}\text{U}$ .

647  
648 The presence of the build-up increases the absorbed dose rate in air and plays an important  
649 role in the final obtained dose received from building materials. In case the build-up is absent,  
650 a decrease in absorbed dose rate in air of 52 %, 50 %, 48 % and 67 % for respectively  $^{238}\text{U}$ ,  
651  $^{232}\text{Th}$ ,  $^{40}\text{K}$  and  $^{235}\text{U}$  is observed. In case of the ISS<sub>Pelli</sub> model, the use of the Pelliccioni Berger  
652 parameters lowered the absorbed dose rate in air with 2.8 % and 2.6 % for respectively  $^{238}\text{U}$   
653 and  $^{232}\text{Th}$  in comparison with the ISS<sub>orig</sub> model, which uses the Berger parameters described  
654 by Markkanen. Further improvements on the accuracy of the B and consequently the  
655 absorbed dose rate in air can be made by working with build-up factors customized towards  
656 the chemical composition of the building material with for example a geometric progression  
657 approach [49].

658  
659  
660  
661  
662

663 The developed EGDA>0% model is complementary to the existing ACI/original Markkanen  
664 model and  $I(\rho d)/D(\rho d)$  index/dose calculations which prove relevant for the dose assessment  
665 within the European legislative framework applicable towards building materials. Due to its  
666 simplicity the authors recommend to perform a first screening by using the ACI proposed by  
667 the EU-BSS in the case of building materials thinner than 20 cm or lighter than 2350 kg/m<sup>3</sup>. In  
668 the case of a building material thicker than 20 cm or heavier than 2350 kg/m<sup>3</sup>, the authors  
669 propose to use D( $\rho d$ ) calculation tool of Nuccetelli et al. [2] in case of standard room sizes. In  
670 case the resulting dose of this calculation exceeds 1 mSv/y one should perform a more  
671 detailed dose assessment. The EGDA>0% model can be used for these specific cases. The  
672 EGDA>0% model also allows coping with non-standard room sizes or the presence of doors  
673 and windows The model does not consider the dose originated by  $^{222}\text{Rn}$  exhalation resulting  
674 in an overestimation of the total external gamma dose originating from building materials.

675  
676 A sensitivity analysis was performed of the EGDA>0% model. The main factors that contribute  
677 to increase the absorbed dose rate in air in comparison to a standard concrete room (Volume  
678 of 56 m<sup>3</sup>; density of 2350kg/m<sup>3</sup>; wall/floor/ceiling thickness of 20 cm) are

- 679 • Increasing density; in case of 3500 kg/m<sup>3</sup> an increase of 9 %, 10 %, 11 % and 2 % for  
680 respectively  $^{238}\text{U}$ ,  $^{232}\text{Th}$ ,  $^{40}\text{K}$  and  $^{235}\text{U}$  is observed.
- 681 • Increasing thickness; in case of 80 cm thick walls an increase of 6 %, 7 %, 8 % and 1 %  
682 for respectively  $^{238}\text{U}$ ,  $^{232}\text{Th}$ ,  $^{40}\text{K}$  and  $^{235}\text{U}$  is observed.
- 683 • Increasing volume; in case of a room volume of 280 m<sup>3</sup> an increase of 5 %, 6 %, 6 %  
684 and 2 % for respectively  $^{238}\text{U}$ ,  $^{232}\text{Th}$ ,  $^{40}\text{K}$  and  $^{235}\text{U}$  is observed.

685  
686 The main factors that contribute to decrease the absorbed dose rate in air in comparison to a  
687 standard concrete room are:

- 688 • Decreasing density; in case of 1000 kg/m<sup>3</sup> a decrease of 34 %, 35 %, 38 % and 20 % for  
689 respectively <sup>238</sup>U, <sup>232</sup>Th, <sup>40</sup>K and <sup>235</sup>U is observed.
- 690 • Decreasing thickness; in case of 5 cm thick walls a decrease of 27 %, 28 %, 29 % and  
691 21 % for respectively <sup>238</sup>U, <sup>232</sup>Th, <sup>40</sup>K and <sup>235</sup>U is observed.
- 692 • Decreasing volume; in case of a volume of 2.8 m<sup>3</sup> a decrease of 4 %, 4 %, 4 % and 3 %  
693 for respectively <sup>238</sup>U, <sup>232</sup>Th, <sup>40</sup>K and <sup>235</sup>U is observed.
- 694 • Presence of windows or doors; in case of one window of 2 x 2 m in wall 1 a decrease  
695 of 4 % for <sup>238</sup>U, <sup>232</sup>Th, <sup>40</sup>K and <sup>235</sup>U is observed.  
696

697 In addition, the shape of the room can also impact the absorbed dose rate in air. Also the  
698 position and size of the window or door in the wall will impact the final absorbed dose rate in  
699 air. Larger windows positioned in the middle of the wall lead to a lower absorbed dose rate in  
700 air. The implementation of the chemical composition in the model via the attenuation  
701 coefficients showed limited effects on the absorbed dose rate in air. For a standard room an  
702 increase of 1.4 %, 0.9 % and 2.1 % is observed for <sup>238</sup>U, <sup>232</sup>Th and <sup>40</sup>K in case of a FSIP sample  
703 composition in comparison to a concrete sample composition. In contrast, a decrease of 6.8%  
704 in case of <sup>235</sup>U is observed.

705 Although the Markkanen room model is widely spread and used as a conservative screening  
706 tool in European legislation, the uncertainty of the method should be assessed. The expansion  
707 proposed here expands the model with validated scientific data but does not take care of the  
708 uncertainty. The uncertainty assessment is a topic for further research.  
709

## 710 Acknowledgement

711

712 This work was supported by the COST Action TU1301. [www.norm4building.org](http://www.norm4building.org).

713

## 714 References

715

- 716 [1] M. Markkanen, Radiation Dose Assessments for Materials with Elevated Natural  
717 Radioactivity, Finish Cent. Radiat. Nucl. Safety. Rep. STUK-B-STO 32. (1995) 1–41.
- 718 [2] C. Nuccetelli, F. Leonardi, R. Trevisi, A new accurate and flexible index to assess the  
719 contribution of building materials to indoor gamma exposure, J. Environ. Radioact.  
720 143 (2015) 70–75. doi:10.1016/j.jenvrad.2015.02.011.
- 721 [3] United Nations, Sources and Effects of Ionizing Radiation United Nations Scientific  
722 Committee on the Effects of Atomic Radiation UNSCEAR 2000 Report to the General  
723 Assembly, with Scientific Annexes VOLUME I: SOURCES, 2000.
- 724 [4] European Council, Laying down basic safety standards for protection against the  
725 dangers arising from exposure to ionising radiation, and repealing directives  
726 89/618/Euratom, 90/641/Euratom, 96/29/Euratom, 97/43/Euratom and  
727 2003/122/Euratom, Off. J. Eur. Union. (2014) 1–73.
- 728 [5] European Commission, A resource-efficient Europe - Flagship initiative under the  
729 Europe 2020 Strategy, (2011).
- 730 [6] European Commission, A strategy for smart, sustainable and inclusive growth, (2010).
- 731 [7] European Commission, Roadmap to a resource efficient Europe, (2011).

- 732 [8] W. Schroeyers, T. Croymans-Plaghki, S. Schreurs, Towards a holistic approach for risk  
733 assessment when reusing slag with enhanced NORM content in building materials, 4th  
734 Int. Slag Valoris. Symp. (2015).
- 735 [9] Y. Pontikes, R. Snellings, Cementitious binders incorporating residues, in: *Handb.*  
736 *Recycl.*, 2014: p. 219–229. doi:10.1016/B978-0-12-396459-5.00016-7.
- 737 [10] C. Nuccetelli, Y. Pontikes, F. Leonardi, R. Trevisi, New perspectives and issues arising  
738 from the introduction of (NORM) residues in building materials: A critical assessment  
739 on the radiological behaviour, *Constr. Build. Mater.* 82 (2015) 323–331.  
740 doi:10.1016/j.conbuildmat.2015.01.069.
- 741 [11] R. Siddique, I.M. Khan, *Supplementary Cementing Materials*, 2011.  
742 doi:10.1017/CBO9781107415324.004.
- 743 [12] D.V. Ribeiro, J.A. Labrincha, M.R. Morelli, Use of Calcined Bauxite Waste as a  
744 Supplementary Cementitious Material: Study of Pozzolan Activity, *J. Mater. Sci. Eng.*  
745 4 (2014) 172–178.
- 746 [13] T. Croymans, I. Vandael Schreurs, M. Hult, G. Marissens, L. Guillaume, H. Stroh, S.  
747 Schreurs, W. Schroeyers, Variation of natural radionuclides in non-ferrous fayalite  
748 slags during a one-month production period, *J. Environ. Radioact.* (2016).
- 749 [14] R. Trevisi, S. Risica, M. D’Alessandro, D. Paradiso, C. Nuccetelli, Natural radioactivity in  
750 building materials in the European Union: A database and an estimate of radiological  
751 significance, *J. Environ. Radioact.* 105 (2012) 11–20.  
752 doi:10.1016/j.jenvrad.2011.10.001.
- 753 [15] L. Koblinger, Calculation of exposure rates from gamma sources in walls of dwelling  
754 rooms, *Health Phys.* 34 (1978) 459–463.
- 755 [16] E. Strandén, Radioactivity of building materials and the gamma radiation in dwellings,  
756 *Phys. Med. Biol.* 24 (1979) 921–930.
- 757 [17] S. Righi, S. Verità, P.L. Rossi, M.F. Maduar, A dose calculation model application for  
758 indoor exposure to two-layer walls gamma irradiation: the case study of ceramic tiles,  
759 *Radiat. Prot. Dosimetry.* 171 (2016) 545–553. doi:10.1093/rpd/ncv476.
- 760 [18] P. de Jong, W. van Dijk, Modeling gamma radiation dose in dwellings due to building  
761 materials., *Health Phys.* 94 (2008) 33–42. doi:10.1097/01.HP.0000278509.65704.11.
- 762 [19] J. Deng, L. Cao, X. Su, Monte Carlo simulation of indoor external exposure due to  
763 gamma-emitting radionuclides in building materials, *Chinese Phys. C.* 38 (2014)  
764 108202. doi:10.1088/1674-1137/38/10/108202.
- 765 [20] M. Zeeshan Anjum, S.M. Mirza, M. Tufail, N.M. Mirza, Z. Yasin, Natural radioactivity in  
766 building materials: dose determination in dwellings using hybrid Monte Carlo-  
767 deterministic approach, *Int. Conf. Nucl. Data Sci. Technol.* (2007) 1–4.  
768 doi:10.1051/ndata:07187.
- 769 [21] N.M. Mirza, S. Mirza, A Shape and Mesh Adaptive Computational Methodology for  
770 Gamma Ray Dose from Volumetric Sources, *Radiat. Prot. Dosimetry.* 38 (1991) 307–  
771 314. doi:10.1093/oxfordjournals.rpd.a081106.
- 772 [22] R. Mustonen, Methods for evaluation of doses from building materials, *Radiat. Prot.*  
773 *Dosimetry.* 7 (1984) 235–238.
- 774 [23] C. Nuccetelli, S. Risica, M.D. Alessandro, R. Trevisi, Natural radioactivity in building  
775 material in the European Union : robustness of the activity concentration index I and  
776 comparison with a room model, *J. Radiol. Prot.* 32 (2012) 349–358. doi:10.1088/0952-  
777 4746/32/3/349.
- 778 [24] V. Manić, G. Manić, D. Nikezic, D. Krstic, Calculation of Dose Rate Conversion Factors

779 for 238U, 232Th and 40K in Concrete Structures of Various Dimensions, With  
780 Application To Nis, Serbia, *Radiat. Prot. Dosimetry*. 152 (2012) 361–368.

781 [25] V. Manić, D. Nikezic, D. Krstic, G. Manić, Assessment of indoor absorbed gamma dose  
782 rate from natural radionuclides in concrete by the method of build-up factors, *Radiat.*  
783 *Prot. Dosimetry*. 162 (2014) 609–617. doi:10.1093/rpd/nct358.

784 [26] B. Chen, Q. Wang, W. Zhuo, Assessment of gamma dose rate in dwellings due to  
785 Decorative stones., *Radiat. Prot. Dosimetry*. 166 (2015) 1–4. doi:10.1093/rpd/ncv256.

786 [27] S. Risica, C. Bolzan, C. Nuccetelli, Radioactivity in building materials: room model  
787 analysis and experimental methods., *Sci. Total Environ*. 272 (2001) 119–126.

788 [28] European Commission, Radiation protection 112 Radiological protection principles  
789 concerning the natural radioactivity of building materials, (1999) 1–16.

790 [29] R. Mustonen, Methods for evaluation of radiation from building materials, *Radiat.*  
791 *Prot. Dosimetry*. 7 (1985) 235–238.

792 [30] European Commission, Radiation protection 122 practical use of the concepts of  
793 clearance and exemption Part II application of the concetps of exemption and  
794 clearance to natural radiation sources, 2002.

795 [31] Laboratoire national Henri Becquerel, Decay Data Evaluation Project, (2016).  
796 <http://www.nucleide.org/DDEP.htm> (accessed May 22, 2016).

797 [32] NIST, Composition of Concrete, Portland, (n.d.) 1. [http://physics.nist.gov/cgi-](http://physics.nist.gov/cgi-bin/Star/compos.pl?matno=144)  
798 [bin/Star/compos.pl?matno=144](http://physics.nist.gov/cgi-bin/Star/compos.pl?matno=144).

799 [33] J.E. Martin, Physics for radiation protection, WILEY-VCH Verlag GmbH & Co. KGaA 2<sup>nd</sup>  
800 Edition, 2006.

801 [34] J.H. Hubbell, S.M. Seltzer, Tables of x-ray mass attenuation coefficients and mass  
802 energy-absorption coefficients 1 keV to 20 meV for elements z = 1 to 92 and 48  
803 additional substances of dosimetric interest, 1995.

804 [35] M. Pelliccioni, Fondamenti fisici della radioprotezione, Pitagora, 1989.

805 [36] D. Krstic, D. Nikezic, Calculation of Indoor Effective Dose factors in Ornl Phantoms  
806 Series Due to Natural Radioactivity in Building Materials, *Health Phys*. 97 (2009) 299–  
807 302.

808 [37] R Development Core Team, R: A language and environment for statistical computing.  
809 R Foundation for Statistical Computing, Vienna, Austria., (2008). [http://www.r-](http://www.r-project.org)  
810 [project.org](http://www.r-project.org).

811 [38] J.H. Hubbell, Photon mass attenuation and energy-absorption coefficients, *Int. J. Appl.*  
812 *Radiat. Isot*. 33 (1982) 1269–1290.

813 [39] M.J. Berger, J.H. Hubbell, S.M. Seltzer, J. Chang, J.S. Coursey, R. Sukumar, D.S. Zucker,  
814 K. Olsen, XCOM: Photon Cross Sections Database, NIST Stand. Ref. Database 8. (2010)  
815 1–5. <http://www.nist.gov/pml/data/xcom/>.

816 [40] IAEA, NuDat, (n.d.). <http://www.nndc.bnl.gov/nudat2/>.

817 [41] L. Kriskova, P.T. Jones, H. Janssen, B. Blanpain, Y. Pontikes, Synthesis and  
818 Characterisation of Porous Inorganic Polymers from Fayalite Slag., *Slag Valoris. Symp.*  
819 *Zero Waste*. 4 (2015) 227–230.

820 [42] S. Onisei, K. Lesage, B. Blanpain, Y. Pontikes, Early Age Microstructural  
821 Transformations of an Inorganic Polymer Made of Fayalite Slag, *J. Am. Ceram. Soc*. 9  
822 (2015) 1–9. doi:10.1111/jace.13548.

823 [43] R.I. Iacobescu, V. Cappuyns, T. Geens, L. Kriskova, S. Onisei, P.T. Jones, Y. Pontikes,  
824 The influence of curing conditions on the mechanical properties and leaching of  
825 inorganic polymers made of fayalitic slag, *Front. Chem. Sci. Eng*. (2017) 208–213.

- 826 doi:10.1007/s11705-017-1622-6.
- 827 [44] M. Berger, J. Hubbell, XCOM: Photon cross sections on a personal computer, Natl. Bur.  
828 Stand. Washington, DC (USA). Cent. Radiat. Res. (1987) 1–28. doi:10.2172/6016002.
- 829 [45] M. Marangoni, L. Arnout, L. Machiels, L. Pandelaers, E. Bernardo, P. Colombo, Y.  
830 Pontikes, C. Jantzen, Porous, Sintered Glass-Ceramics from Inorganic Polymers Based  
831 on Fayalite Slag, J. Am. Ceram. Soc. 99 (2016) 1–7. doi:10.1111/jace.14224.
- 832 [46] T. Hertel, B. Blanpain, Y. Pontikes, A Proposal for a 100 % Use of Bauxite Residue  
833 Towards Inorganic Polymer Mortar, J. Sustain. Metall. 2 (2016) 394–404.  
834 doi:10.1007/s40831-016-0080-6.
- 835 [47] IAEA, Extent of Environmental Contamination by Naturally Occurring Radioactive  
836 Material (NORM) and Technological Options for Mitigation - Technical reports series  
837 no. 419, 2003.
- 838 [48] T. Croymans, I. Schreurs, M. Hult, G. Marissens, H. Stroh, G. Lutter, S. Schreurs, W.  
839 Schroyers, Variation of natural radionuclides in non-ferrous fayalite slags during a  
840 one-month production period, J. Environ. Radioact. 172 (2017) 63–73.  
841 doi:10.1016/j.jenvrad.2017.03.004.
- 842 [49] Y. Harima, Validity of the Geometric-Progression Formula in approximating Gamma-  
843 Ray Buildup Factors, Nucl. Sci. Eng. 5 (1986) 24–35.
- 844